

# Lossless Negative Refraction in An Active Dense Gas of Atoms

Peter P. Orth, Jörg Evers, and Christoph H. Keitel

Max-Planck Institut für Kernphysik, Saupfercheckweg 1, 69117 Heidelberg, Germany

(Dated: February 2, 2008)

Current designs for negative index materials are passive, such that they suffer from significant losses that prohibit applications, in particular towards optical frequencies. We predict, based on nonlinear optical Bloch equations, negative refraction with zero absorption in an active, i.e., amplifying, dense gas of atoms. External laser fields are used to tune the medium's electromagnetic response and an additional weak pumping field controls its absorption properties. Metastable Neon is identified as a suitable experimental candidate at infrared frequencies to implement a lossless active negative index material.

Over the past years, tremendous progress has been accomplished in the field of negative refraction mostly related to the ongoing miniaturization of artificial structures [1, 2]. In such metamaterials, negative refraction is accompanied by a substantial amount of absorption especially towards higher frequencies. These losses typically occur since the refractive index becomes negative only close to electromagnetic resonances where the absorption is high. All known metamaterials are passive devices and recent proposals to include gain materials to compensate for losses have not yet been successfully realized [3]. As a result, the relevant figure of merit, the ratio between the real and the imaginary part of the refractive index  $FOM = |\text{Re}(n)/\text{Im}(n)|$  for high-frequency metamaterials is currently only of the order unity, prohibiting most of the possible applications [4, 5, 6, 7, 8]. As a different approach, recently, negative refraction without metamaterials has been proposed in dense gases of atoms [9, 10, 11]. Gases naturally have a macroscopic extend in all spatial dimensions, unlike high-frequency metamaterials which typically are produced layer by layer on a surface [12]. The proposed systems, however, have in common with current metamaterials that they are also passive and lossy.

In this Letter, we demonstrate how truly lossless negative refraction in an active, i.e., amplifying negative index medium can be realized. A dense gas of atoms is exposed to control laser fields that create coherence between different internal atomic states. Quantum interference effects reduce the absorption in the gas and an additional weak incoherent pumping field is used to render the system completely lossless:  $\text{Im}(n) = 0$ ; or transfer it into an active, amplifying state where  $\text{Im}(n) < 0$ . Changing the intensity of the pumping field continuously allows for a controlled transition from a passive to an active state.

We employ nonlinear Bloch equations [13] to account for dipole-dipole interactions, which goes beyond standard local field corrections used in this context so far [11]. The feasibility of our scheme is demonstrated for the case of metastable Neon, where we find negative refraction in the infrared range at a wavelength of about  $\lambda = 5\mu\text{m}$ . The required energy level scheme (see Fig. 1), could also be realized in other atomic species or solid state systems

like doped semiconductors or quantum dot arrays.

Negative refraction occurs if both the electric and the magnetic component of an electromagnetic probe wave couple near-resonantly to the system. Thus, in atomic gases, near-degenerate electric and magnetic dipole transitions are required. The level structure of metastable Neon features such a pair of near-degenerate dipole transitions, see Fig. 1 [10]. Additional laser fields with electric component  $\mathbf{E}_a$  and  $\mathbf{E}_c$  greatly enhance the magnetic response, since they prepare a coherence on the magnetic probe transition. We are interested in the linear response of the medium to the weak probe field of frequency  $\omega_b$  with electric component  $\mathbf{E}_b$  and magnetic field component  $\mathbf{H}_b$ . The induced electric polarization  $\mathbf{P}$  and

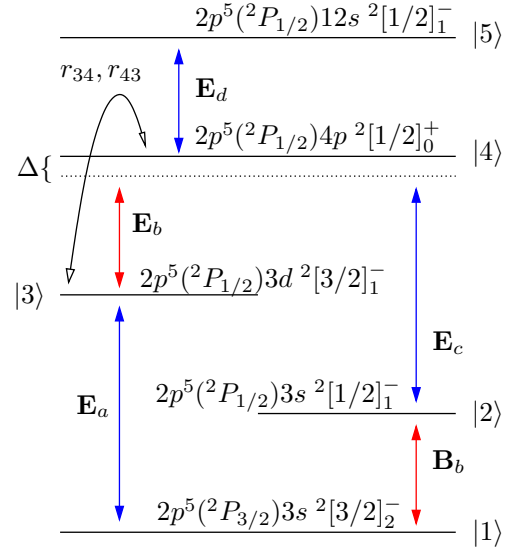


FIG. 1: (Color online) Five-level scheme with probe field  $\mathbf{E}_b$ ,  $\mathbf{B}_b$  (red) and coupling fields  $\mathbf{E}_a$ ,  $\mathbf{E}_c$ ,  $\mathbf{E}_d$  (blue) of frequencies  $\omega_b$ ,  $\omega_a$ ,  $\omega_c$  and  $\omega_d$ , respectively. The electronic states in jL-coupling notation refer to the special case of metastable Neon [14], with corresponding wavelengths  $\lambda_b = 5.4\mu\text{m}$ ,  $\lambda_a = 704\text{nm}$ ,  $\lambda_c = 352\text{nm}$  and  $\lambda_d = 1.05\mu\text{m}$ . The magnetic and electric probe field transitions  $|1\rangle - |2\rangle$  (M1) and  $|3\rangle - |4\rangle$  (E1) are energetically degenerate up to a small energy gap  $\Delta = 3.33\text{cm}^{-1}$ . An incoherent light field (black) acts as a pump rate  $r_{34}$ ,  $r_{43}$  between states  $|3\rangle$  and  $|4\rangle$ .

magnetization  $\mathbf{M}$  at the frequency  $\omega_b$  are given by [15]

$$\begin{aligned}\mathbf{P} &= \chi_{EE}(\omega_b)\mathbf{E}_b + \xi_{EH}(\omega_b)\mathbf{H}_b/4\pi \\ \mathbf{M} &= \chi_{HH}(\omega_b)\mathbf{H}_b + \xi_{HE}(\omega_b)\mathbf{E}_b/4\pi,\end{aligned}\quad (1)$$

where  $\chi_{EE}$ ,  $\chi_{HH}$  are the electric and magnetic susceptibilities, respectively, and  $\xi_{EH}$ ,  $\xi_{HE}$  are so-called chirality coefficients that describe the cross-coupling between electric and magnetic fields in a chiral medium. The refractive index depends on the probe wave polarization and we obtain for circular  $\sigma^\pm$ -polarization [15]

$$n_\pm = \sqrt{\varepsilon\mu - \frac{(\xi_{EH} + \xi_{HE})^2}{4}} \pm \frac{i}{2}(\xi_{HE} - \xi_{EH}), \quad (2)$$

where we have defined the electric permittivity  $\varepsilon = 1 + 4\pi\chi_{EE}$  and the magnetic permeability  $\mu = 1 + 4\pi\chi_{HH}$  in the usual way.

To find the linear response coefficients  $\chi_{\alpha\alpha}$  and  $\xi_{\alpha\beta}$  ( $\alpha \neq \beta \in \{E, H\}$ ), we consider the time-evolution of a single five-level atom with density matrix  $\rho$  which is governed by the Master equation [16]

$$\dot{\rho} = \frac{1}{i\hbar}[H, \rho] - \sum_{j,k} \frac{\gamma_{jk}}{2} (|j\rangle\langle j|\rho + \rho|j\rangle\langle j| - 2|k\rangle\langle j|\rho|j\rangle\langle k|), \quad (3)$$

with the system Hamiltonian given by

$$\begin{aligned}H &= \sum_{j=1}^5 \epsilon_j |j\rangle\langle j| + \frac{1}{2} \{ -\boldsymbol{\mu}_{21} \cdot \mathbf{B}_L e^{-i\omega_b t} |2\rangle\langle 1| \\ &\quad - \mathbf{d}_{43} \cdot \mathbf{E}_L e^{-i\omega_b t} |4\rangle\langle 3| - \hbar\Omega_{31} e^{-i\omega_a t} |3\rangle\langle 1| \\ &\quad - \hbar\Omega_{42} e^{-i\omega_c t} |4\rangle\langle 2| - \hbar\Omega_{54} e^{-i\omega_d t} |5\rangle\langle 4| + \text{h.c.} \}.\end{aligned}\quad (4)$$

Here,  $\epsilon_j$  is the energy of state  $|j\rangle$  and the other terms describe the interaction with the laser fields in the long-wavelength and dipole approximations. The fields have frequencies  $\omega_i$  with  $i \in \{a, b, c, d\}$ . The laser detuning on transition  $|i\rangle - |j\rangle$  reads simply  $\hbar\delta_{ij} = \hbar\omega_{ij} + \epsilon_{ij}$ , where  $\omega_{ij} = \omega_i - \omega_j$  and  $\epsilon_{ij}$  accordingly, if we introduce the following combination of angular frequencies  $\omega_1 = \omega_c + \omega_d + \omega_b$ ,  $\omega_2 = \omega_c + \omega_d$ ,  $\omega_3 = \omega_b + \omega_c + \omega_d - \omega_a$ ,  $\omega_4 = \omega_d$ ,  $\omega_5 = 0$ . The electric control field components  $\mathbf{E}_i = \frac{E_i}{2}\boldsymbol{\varepsilon}_i e^{-i\omega_i t} + \text{c.c.}$  with polarization vector  $\boldsymbol{\varepsilon}_i$  ( $i \in \{a, c, d\}$ ) give rise to the complex Rabi frequencies  $\Omega_{31} = \mathbf{d}_{31} \cdot \mathbf{E}_a/\hbar$ ,  $\Omega_{42} = \mathbf{d}_{42} \cdot \mathbf{E}_c/\hbar$ ,  $\Omega_{54} = \mathbf{d}_{54} \cdot \mathbf{E}_d/\hbar$ , where  $\mathbf{d}_{ij} = \langle i|\mathbf{d}|j\rangle$  is the electric dipole operator between states  $|i\rangle$  and  $|j\rangle$ . Note that the Hamiltonian Eq. (4) contains instead of the external probe fields  $\mathbf{E}_b$ ,  $\mathbf{H}_b$  the actual (local) fields inside the medium  $\mathbf{E}_L = \mathbf{E}_b + \frac{4\pi}{3}\mathbf{P}$ ,  $\mathbf{H}_L = \mathbf{H}_b + \frac{4\pi}{3}\mathbf{M}$  [17]. This accounts for dipole-dipole interactions which cannot be neglected for large atomic densities.

The second part of the master equation describes the spontaneous decay of excited states and the decoherence that arises due to elastic collisions. The decay rate on

transition  $|i\rangle - |j\rangle$  is denoted by  $\gamma_{ij}$  and set to  $\gamma_{ij} = \gamma$ , if  $|i\rangle - |j\rangle$  is electric dipole allowed (E1) and set to  $\gamma_{ij} = \alpha^2\gamma$  for metastable E2, M1 transitions, where  $\alpha = 1/137$  is the fine-structure constant. A typical decay rate in metastable Neon in angular frequencies is  $\gamma = 10^7 \frac{\text{rad}}{\text{s}}$ . To include the effect of elastic collisions, we add a collisional decay constant  $\gamma_C$  to the decay rates of the off-diagonal density matrix elements:  $\tilde{\gamma}_{xy} = \sum_j (\gamma_{xj} + \gamma_{yj})/2 + \gamma_C$  ( $x \neq y \in \{1, \dots, 5\}$ ). In the following, we set  $\gamma_C = \gamma$ . A numerical analysis shows that our system is quite robust against changes in the decay rates. In particular, our model does not rely on the preservation of an electromagnetically induced transparency ground state coherence as in previous models [11], which is challenging in particular at high particle densities.

The steady-state coherences  $\rho_{43}$  and  $\rho_{21}$  determine the induced polarization and magnetization at the probe field frequency as  $\mathbf{P} = N(\rho_{43}\mathbf{d}_{34} + \text{c.c.})$  and  $\mathbf{M} = N(\rho_{21}\boldsymbol{\mu}_{12} + \text{c.c.})$ , where  $N$  is the density of atoms, and  $\boldsymbol{\mu}_{12} = \langle 1|\boldsymbol{\mu}|2\rangle$  is the magnetic dipole moment of the M1-transition. It turns out that large atom densities are required to obtain negative refraction, meaning that many particles are found in a cubic wavelength volume  $N\lambda^3 \gg 1$ . Under such conditions, the local probe fields  $\mathbf{E}_L$ ,  $\mathbf{H}_L$  inside the medium may considerably deviate from the externally applied probe fields  $\mathbf{E}_b$ ,  $\mathbf{H}_b$  in free space, since they contain contributions from neighboring atoms. The fields are related by the Lorentz-Lorenz (LL) formulas [17]:  $\mathbf{E}_L = \mathbf{E}_b + \frac{4\pi}{3}\mathbf{P}$  and  $\mathbf{H}_L = \mathbf{H}_b + \frac{4\pi}{3}\mathbf{M}$ . Different approaches have been proposed in the literature to solve this problem. We found the simplest approach, which is expected to be valid for moderate densities and consists of expanding the steady-state density matrix elements  $\rho_{21}$  and  $\rho_{43}$  to linear order in the local fields  $\mathbf{E}_L$ ,  $\mathbf{H}_L$  and only then substitute the external fields for the local fields using the LL-relations, to be insufficient to describe our system. Therefore, we relate the local fields via the LL-relations to the external fields already in the density matrix equations of motion [13] and obtain a set of non-linear equations. This has the advantage that in the framework of the LL-formulas the local field effects are treated without approximations. Since the equations are non-linear, however, one typically requires a numerical analysis.

We numerically integrate the nonlinear equations until the system has reached its steady state for (twenty) different electric field amplitudes  $E_b$ , holding the magnetic field amplitude  $H_b$  fixed. Linear regression of the relevant coherences  $\rho_{21}, \rho_{43}$  as a function of  $E_b$  allows to extract the response coefficients as slope and y-axis intercept from Eqs. (1). We note that in the case of a circularly polarized probe field, these equations describe scalar relations, since  $\mathbf{H}_b = \mathbf{B}_b = \mp i\mathbf{E}_b$  for  $\sigma^\pm$ -polarization. In particular for the electric polarization

$$\mathbf{P} = \frac{P}{2}\boldsymbol{\varepsilon}_b e^{-i\omega_b t} + \text{c.c.} = N(\tilde{\rho}_{43} e^{-i\omega_b t} \mathbf{d}_{34} + \text{c.c.}), \quad (5)$$

where  $\tilde{\rho}_{43} = \rho_{43}e^{i\omega_b t}$  is the slowly varying part of the coherence, we obtain for a  $\sigma^-$ -polarized probe field

$$P = 2N\tilde{\rho}_{43}d_{34} = \chi_{EE}\frac{\hbar\gamma w_E}{d_{43}} + \xi_{EH}\frac{i\hbar\gamma w_B}{4\pi\mu_{21}}, \quad (6)$$

with the small expansion parameters  $w_E = d_{43}E_b/\hbar\gamma$  and  $w_B = \mu_{21}B_b/\hbar\gamma$ . The dipole moments  $d_{ij}$  and  $\mu_{ij}$  can be evaluated via the respective spontaneous decay rates as  $\sqrt{3\gamma_{ij}\hbar c^3/(4\omega_{ij}^3)}$ . By linear regression of  $P(w_E) = m_P w_E + b_P$  one finds

$$\chi_{EE} = \frac{d_{43}m_P}{\hbar\gamma}, \quad \xi_{EH} = -\frac{4\pi i\mu_{21}b_P}{\hbar\gamma w_B}. \quad (7)$$

Analogously, one obtains the response coefficients for the magnetization  $M = m_M w_E + b_M$ :

$$\chi_{HH} = -\frac{i\mu_{21}b_M}{\hbar\gamma w_B}, \quad \xi_{HE} = \frac{4\pi d_{43}m_M}{\hbar\gamma}. \quad (8)$$

It turns out that the chirality coefficients depend on the relative phase of the applied laser fields. Since they are typically several orders of magnitude smaller than the direct coefficients  $\varepsilon$  and  $\mu$ , however, they do not contribute significantly to the index of refraction. Still, in our calculations we average over this phase to simulate an experiment without phase control, which effectively reduces the magnitude of  $\xi_{EH}$  and  $\xi_{HE}$  almost to zero.

In our setup, the coupling laser fields serve different purposes: the fields  $\mathbf{E}_a$  and  $\mathbf{E}_c$  enhance the magnetic response by inducing the coherence  $\rho_{21}$  which drives the magnetic dipole moment of the atom. We choose the frequencies of both fields to be equal  $\omega_a = \omega_c$  and almost resonant with the transition  $|1\rangle - |3\rangle$ :  $\delta_{31} \ll \Omega_{31}$  [18]. The third laser field  $\mathbf{E}_d$  is resonant with the transition  $|4\rangle - |5\rangle$  ( $\delta_{54} = 0$ ), causing an Autler-Townes-splitting of the fourth level into two dressed states at  $\epsilon_4 \rightarrow \epsilon_4 \pm \hbar|\Omega_{54}|/2$ . Thereby, electric and magnetic probe field resonances are shifted with respect to each other. For zero field, they are separated in Neon by the gap  $\Delta = (\epsilon_{43} - \epsilon_{21})/\hbar = 3.33 \text{ cm}^{-1} = 100 \text{ GHz} = 2\pi \cdot 10^4 \gamma$ , since  $\gamma = 10^7/(2\pi) \text{ Hz}$  is a typical value for the spontaneous decay rate in Neon. Note that in angular frequencies this corresponds to  $\gamma = 10^7 \frac{\text{rad}}{\text{s}}$ . In order to close the gap, one has to apply a strong laser field with  $\Omega_{54} \approx 10^4 \gamma$ . Yet we find that neighboring transitions are still detuned at the least by  $15 \Omega_{54}$ , making such large light shifts feasible without inducing unwanted transitions. Thus the field  $\Omega_{54}$  allows to circumvent the problem of non-degenerate electric and magnetic probe field transition [9]. It is important to note, however, that it is not mandatory to close this gap completely, because the states  $|2\rangle$  and  $|3\rangle$  are connected by a two-photon transition induced by the fields  $\mathbf{E}_c$  and  $\mathbf{E}_b$  which becomes important for nonzero gap frequencies  $\Delta$ .

This two-photon transition is the motivation to apply in addition an incoherent light field resonant with the

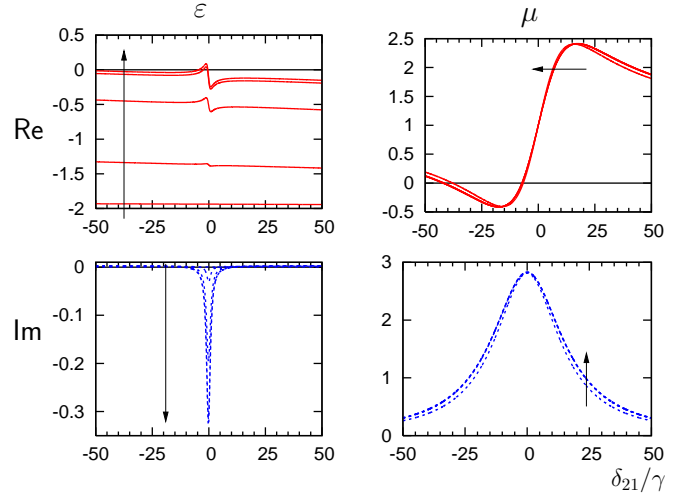


FIG. 2: (Color online) Electric permittivity  $\varepsilon$  and magnetic permeability  $\mu$  as a function of  $\delta_{21}$  for different pump rates  $r_1 = 0$ ,  $r_2 = 0.2512$ ,  $r_3 = 1$ ,  $r_4 = 1.679$ ,  $r_5 = 1.698$ ,  $r_6 = 1.799$  (in units of  $10^{-2}\gamma$ ) between states  $|3\rangle$  and  $|4\rangle$ . The arrow denotes the direction of increased pumping. Other parameters are set to  $\Omega_{42} = 5.6$ ,  $\Omega_{31} = 6.3 \cdot 10^{-3}$ ,  $\Delta' = 560$ ,  $\delta_{31} = -10^{-2}$ ,  $\delta_{54} = 0$  (all in units of  $\gamma$ ). The probe field wavelength is  $\lambda = 5 \mu\text{m}$  and the density  $N = 2.5 \cdot 10^{17} \text{ cm}^{-3}$ .

transition  $|3\rangle - |4\rangle$ , which transfers population between the levels with rates  $r_{34} = r_{43} = r$  changing the decay rates from  $\gamma_{43} \rightarrow \gamma_{43} + r_{43}$  and accordingly for  $\gamma_{34}$ . Together with spontaneous emission from  $|4\rangle$  to  $|2\rangle$ , it effectively pumps population into  $|2\rangle$ . One finds that for  $\rho_{22} > \rho_{33}$  the probe field is amplified by means of the two-photon process, since it is more likely for the transition to occur in the direction  $|2\rangle \rightarrow |3\rangle$ . This direction involves the emission of a probe field photon and we observe gain in the electric probe field component. Since we choose the laser frequencies  $\omega_a = \omega_c$ , this two-photon resonance is always located at the position of the magnetic probe field resonance which occurs at  $\delta_{21} = 0$ . The two-photon virtual intermediate level is separated from  $|4\rangle$  by the effective gap  $\Delta' = -\Delta + \Omega_{54}/2$ . If we choose  $\Delta'$  sufficiently large, the two-photon transition will be the dominant process around zero probe detuning.

In Figure 2, the permittivity and the permeability of the medium are shown as a function of the probe field detuning from the magnetic resonance  $\delta_{21}$ . The resulting refractive index can be seen in Fig. 3. Without incoherent pumping the system is passive and thus  $\varepsilon$ ,  $\mu$  and  $n$  have a positive imaginary part, i.e., the medium absorbs. Whereas absorption is small for the electric response due to local field effects, the losses are significant in the magnetic component. We observe power broadening in all response functions due to the nonlinearities that appear in the master equation to include near-dipole-dipole effects. Gradually increasing the incoherent pumping rate, we find that the imaginary part of  $\varepsilon$  around zero detun-

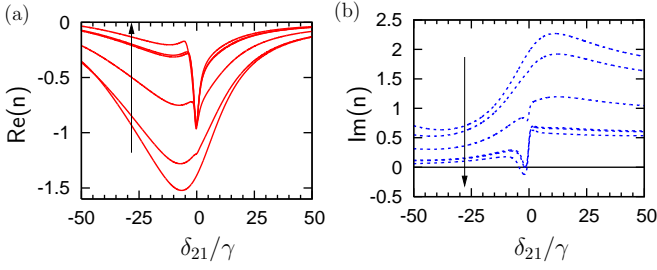


FIG. 3: (Color online) Refractive index  $n$  for different pump rates as a function of  $\delta_{21}$ . The parameters are the same as in Fig. 2. Arrows indicate the direction of increased pumping. Without pumping, the imaginary part is strictly positive, as expected for a passive system. On increasing the pump rate, the system turns active, and negative refraction is obtained without absorption or even with amplification.

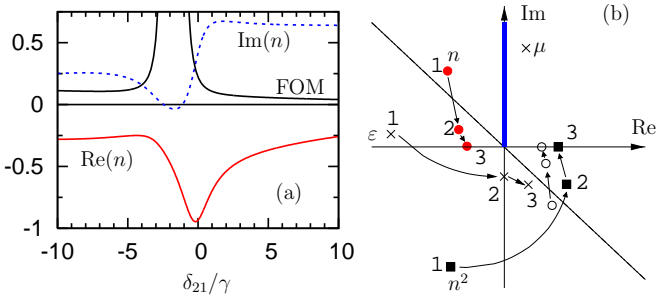


FIG. 4: (Color online) (a) Lossless negative refraction for a pump rate of  $r = 1.718 \cdot 10^{-2} \gamma$ .  $\text{Re}(n)$  (solid red line),  $\text{Im}(n)$  (dashed blue line), figure of merit  $\text{FOM} = |\text{Re}(n)/\text{Im}(n)|$  (solid black line). (b) Paths of  $\epsilon$ ,  $\mu$ ,  $n^2$ , and  $\pm\sqrt{n^2}$  in the complex plane parameterized by the pumping rate  $r$ . Step 1 corresponds to zero pumping  $r_1$ , the system is in a passive state and the physical solution is denoted by a filled circle (red). Increasing the pump rate continuously, we follow the path indicated by the arrow. Step 2 is at an intermediate pump rate in Fig. 3, where the system is still absorptive. Finally, step 3 corresponds to lossless negative refraction.

ing turns negative, indicating that the two-photon transition  $|2\rangle - |3\rangle$  amplifies the probe field. The magnetic permeability is mostly unaffected by the incoherent field. The real part of  $n$  is negative for all detunings, which even includes regions of positive  $\text{Re}(\mu)$ , but absorption is dominant there. Without pumping, the imaginary part is strictly positive, as expected for a passive system.

Increasing the pump rate  $r$  decreases the absorption over the whole range of displayed probe detunings. Finally, negative refraction occurs without absorption or even with amplification, see Fig. 4(a). In this frequency range, the FOM becomes very large due to the vanishing imaginary part. The crossover from passive to active induced by the incoherent pumping can easily be understood by following the path of  $\epsilon$ ,  $\mu$ ,  $n^2$  and  $n$  in the complex plane as a function of the pump rate  $r$ , see Fig. 4(b). Without pumping (step 1), the system is pas-

sive and shows significant absorption ( $\text{FOM} < 1$ ). Increasing the pump rate, the imaginary part of  $\epsilon$  becomes negative which compensates for the losses via the magnetic component. The imaginary part of the refractive index decreases ( $\text{FOM} \gg 1$ ) and finally vanishes, while the real part remains negative. Thus negative refraction with a large figure of merit can even occur for positive  $\text{Re}(\epsilon, \mu)$  if  $|\text{Im}(\epsilon, \mu)| \neq 0$  and the losses via the magnetic field component are compensated by gain via the electric component. Since we can continuously change the pump rate, we can identify the physically correct branch if we follow the path in the complex plane starting from the root with positive imaginary part for the passive system.

To summarize, we have predicted negative refraction with truly zero loss in a dense gas of atoms. Employing the transition to an active medium by means of an incoherent pumping field allows to study a qualitatively new parameter range not accessible with current devices. Due to its wide tunability and control, our system is not only interesting from a proof-of-principle point of view, but also promises the enhancement of optical effects which are severely degraded by losses accompanying negative refraction in current metamaterials.

- 
- [1] V. G. Veselago and E. E. Narimanov, *Nature Materials* **5**, 759 (2006).
  - [2] V. M. Shalaev, *Nature Photonics* **1**, 41 (2007).
  - [3] A. D. Boardman, Y. G. Rapoport, N. King, and V. N. Malnev, *J. Opt. Soc. Am. B* **24**, A53 (2007).
  - [4] R. A. Shelby, D. R. Smith, and S. Schultz, *Science* **292**, 77 (2001).
  - [5] H. J. Lezec, J. A. Dionne, and H. A. Atwater, *Science* **316**, 430 (2007).
  - [6] E. E. Narimanov and V. A. Podolsky, *Opt. Lett.* **30**, 75 (2005).
  - [7] D. R. Smith, D. Schurig, M. Rosenbluth, S. Schultz, S. A. Ramakrishna, and J. B. Pendry, *Appl. Phys. Lett.* **82**, 1506 (2003).
  - [8] R. Merlin, *Appl. Phys. Lett.* **84**, 1290 (2004).
  - [9] M. O. Oktel and O. E. Müstecaplıoglu, *Phys. Rev. A* **70**, 053806 (2004).
  - [10] Q. Thommen and P. Mandel, *Phys. Rev. Lett.* **96**, 053601 (2006).
  - [11] J. Kästel, M. Fleischhauer, S. F. Yelin, and R. L. Walsworth, *Phys. Rev. Lett.* **99**, 073602 (2007).
  - [12] G. Dolling, M. Wegener, and S. Linden, *Opt. Lett.* **32**, 551 (2007).
  - [13] C. M. Bowden and J. P. Dowling, *Phys. Rev. A* **47**, 1247 (1993).
  - [14] <http://physics.nist.gov/Pubs/AtSpec/>;  
<http://physics.nist.gov/PhysRefData/>.
  - [15] J. B. Pendry, *Science* **306**, 1353 (2004).
  - [16] M. O. Scully and M. S. Zubairy, *Quantum Optics* (Cambridge, 1997).
  - [17] J. D. Jackson, *Classical Electrodynamics* (John Wiley & Sons, 1998).
  - [18] M. Mahmoudi and J. Evers, *Phys. Rev. A* **74**, 063827 (2006).

(2006).